Brambilla Vittoria (Orcid ID: 0000-0003-0673-6898)

Rice florigens control a common set of genes at the shoot apical meristem including the F-BOX BROADER TILLER ANGLE 1 that regulates tiller angle and spikelet development

Lorenzo Mineri[2*], Martina Cerise[2,3*], Francesca Giaume[1,2], Giulio Vicentini[1], Damiano Martignago[2], Matteo Chiara[2], Francesca Galbiati[2], Alberto Spada[1], David Horner[2], Fabio Fornara[2] and Vittoria Brambilla[1].

1) Department of Agricultural and Environmental Sciences, University of Milan, via Celoria 2, 20133 Milan, Italy
2) Department of Biosciences, University of Milan, via Celoria 26, 20133 Milan, Italy
3) Present address: Max Planck Institute for Plant Breeding Research, Carl Von Linne Weg 10, 50829 Cologne, Germany

*these authors contributed equally

Corresponding author: vittoria.brambilla@unimi.it tel +390250314817

SUMMARY

Rice flowering is triggered by transcriptional reprogramming at the shoot apical meristem (SAM) mediated by florigenic proteins produced in leaves in response to changes in photoperiod. Florigens are more rapidly expressed under short days (SDs) compared to long days (LDs) and include the HEADING DATE 3a (Hd3a) and RICE FLOWERING LOCUS T1 (RFT1) Phosphatidyl Ethanolamine Binding Proteins. Hd3a and RFT1 are largely redundant at converting the SAM into an inflorescence, but whether they activate the same target genes and convey all photoperiodic information that modifies gene expression at the SAM is currently unclear.

We uncoupled the contribution of Hd3a and RFT1 to transcriptome reprogramming at the SAM by RNA-sequencing of dexamethasone-inducible over-expressors of single florigens and wild type plants exposed to photoperiodic induction.

Fifteen highly differentially expressed genes common to Hd3a, RFT1 and SDs were retrieved, ten of which still uncharacterized. Detailed functional studies on some candidates revealed a role for

This article has been accepted for publication and undergone full peer review but has not been through the copyediting, typesetting, pagination and proofreading process which may lead to differences between this version and the Version of Record. Please cite this article as doi: 10.1111/tpj.16345

LOC_Os04g13150 in determining tiller angle and spikelet development and the gene was renamed *BROADER TILLER ANGLE 1* (*BRT1*).

We identified a core set of genes controlled by florigen-mediated photoperiodic induction and defined the function of a novel florigen target controlling tiller angle and spikelet development.

Key words Florigens, Photoperiodic Flowering, Rice, Shoot Apical Meristem, Tiller Angle

INTRODUCTION

Flowering depends upon expression of florigenic proteins in the leaves, which occurs after plants measure favorable environmental conditions and trigger the reproductive phase at the right time of the year. All species that depend upon the photoperiod to measure seasonal cues express florigenic proteins that are members of the Phosphatidyl Ethanolamine Binding Protein (PEBP) family, including FLOWERING LOCUS T (FT) in *Arabidopsis thaliana* and HEADING DATE 3a (Hd3a) and RICE FLOWERING LOCUS T1 (RFT1) in *Oryza sativa* (rice). Features of every florigen include 1) photoperiod dependent expression, which is localized in specific phloematic cells of the leaf veins, 2) translocation to the shoot apical meristem (SAM) and 3) formation of higher order transcriptional complexes (Floral Activation Complexes -FACs) that regulate gene expression during transition of the SAM to reproductive growth (Tamaki et al., 2007; Corbesier et al., 2007; Taoka et al., 2011; Chen et al., 2018; Cerise et al., 2021).

Hd3a and RFT1 belong to a family of 19 rice PEBP and are encoded by paralogous genes located 11 kb apart on chromosome 6 (Karlgren *et al.*, 2011). They share 91% sequence identity but previous studies have highlighted differences in the regulation and function of each of the florigen-features listed above. In Nipponbare, *Hd3a* and *RFT1* transcription in phloematic cells of the leaf veins responds to photoperiod thanks to the activity of many common activators and repressors (Shrestha *et al.*, 2014) However, while *Hd3a* can only be induced under short days (SDs), *RFT1* can also be expressed after a prolonged time of growth under LDs and is responsible for LD flowering (Karlgren et al., 2011; Izawa et al., 2002; Kojima et al., 2002). The B-type response regulator *EARLY HEADING DATE 1* (*Ehd1*) is a common activator of *Hd3a* and *RFT1* in leaves but, while *Hd3a* expression fully depends upon *Ehd1*, *RFT1* might also be activated by other pathways (Zhao *et al.*, 2015).

Hd3a and RFT1 are largely redundant as plants in which both *Hd3a* and *RFT1* expression is reduced by RNAi are unable to flower (Komiya *et al.*, 2008). But, consistently with their different induction

under SD and LD, the single *hd3a* RNAi or mutant is late flowering under SD while *rft1* RNAi or mutant flowers late under LD only (Komiya *et al.*, 2009; Song *et al.*, 2017; Liu *et al.*, 2019).

Differences between Hd3a and RFT1 have also been observed for translocation in the phloem and FAC formation. Interaction of RFT1 with *Oryza sativa* FT-INTERACTING PROTEIN1 (OsFTIP1) is necessary for RFT1 export from phloem companion cells into sieve elements under LDs, suggesting a possible specificity for phloem loading (Song *et al.*, 2017). A similar mechanism has been proposed for Hd3a, whose interaction with OsFTIP9, a homologue of OsFTIP1, mediates its loading in the phloematic stream under SDs (Zhang L, 2022).
When florigens reach the SAM, two molecules bind to a dimer of GF14 proteins to form tetramers that are translocated into the nucleus and subsequently bind to two OsFD1 bZIP transcription factors, thus forming an heterohexamer (Taoka et al., 2011; Peng et al., 2021) .

The florigen-GF14-OsFD1 complex is a FAC empowered with DNA binding functions by the bZIP transcription factor, and binds to the promoter sequences of target genes, required to start inflorescence development (Taoka et al., 2011) . Direct binding of OsFD1 was shown to occur *in vitro* on a C-box element-containing oligomer (*GACGTC*) present in the promoter of the target gene *OsMADS15* (Taoka et al., 2011). Genome-wide studies performed through DAP-Seq identified additional targets, albeit *OsMADS15* promotor sequences were not identified in the datasets (Cerise et al., 2021). After the FAC model was proposed, several works have shown that additional bZIPs can form alternative FACs and that these could involve specifically one or both florigens. Also, some bZIP-florigen interactions did not require the GF14 bridge (Tsuji et al., 2013; Cerise et al., 2021; Kaur et al., 2021) . The flowering repressors bZIPs Hd3a BINDING FACTOR 1 (HBF1) and HBF2 form dimers with Hd3a but need GF14c to interact with RFT1 and reduce FAC target genes expression (Brambilla et al., 2017; Cerise et al., 2021) The bZIP OsFD4 can directly interact with both Hd3a and RFT1 to induce FAC targets expression.
Another group of PEBP involved in flowering includes the four RICE CENTRORADIALIS (RCN1-4). These are closely related to snapdragon CENTRORADIALIS (CEN) and Arabidopsis TERMINAL FLOWER 1 (TFL1) (Bradley *et al.*, 1996; Nakagawa *et al.*, 2002; Conti & Bradley, 2007) and are often referred to as antiflorigens since they display antagonistic functions to the florigens in many species by delaying the transition to reproductive growth (Ahn et al., 2006; Huang et al., 2012; Baumann et al., 2015; Kaneko-Suzuki et al., 2018; Lee et al., 2019).
RCN genes are mainly expressed in the vasculature under both LD and SD conditions, but their proteins move to and accumulate in the SAM during reproductive development (Kaneko-Suzuki et al., 2018). RCN4 at least is also transcribed in the developing panicle (Zhu *et al.*, 2022). At the

molecular level, RCNs have an antagonistic function to Hd3a and RFT1 since they compete for GF14 binding to form Florigen Repressive Complexes (FRC) (Kaneko-Suzuki et al., 2018). FAC and FRC balance gene expression to achieve correct panicle development.

Flowering requires the synchronization of different developmental processes in distinct cell populations. The change of identity of the SAM during the reproductive transition occurs in parallel to the elongation of the culms. We have previously shown that the florigens mediate the increase of GA sensitivity of the stem via reduction of *PREMATURE INTERNODE ELONGATION 1* (*PINE1*) expression, that results in internodes and culm elongation (Gómez-Ariza *et al.*, 2019). We therefore might expect that many developmental processes linked to flowering are regulated by FACs, predominantly composed by one of the two florigens that trigger transcriptional changes in specific sites.

Several experiments have already been performed with the aim of quantifying changes in gene expression upon changes in day length during the floral transition (Furutani *et al.*, 2006; Kobayashi *et al.*, 2012b; Tamaki *et al.*, 2015b; Gómez-Ariza *et al.*, 2019). However, none of these experiments could separate the effect of each florigen at the SAM from that of the full photoperiodic induction. An accurate dissection of the molecular pathways modulated by Hd3a or RFT1 becomes relevant following the consideration that Hd3a and RFT1 have non-equivalent roles during floral induction, and it could be assumed they target a common set of genes, but possibly also genes specific to either of them only.

To separate the effect of Hd3a or RFT1 florigenic signals at the SAM, small portions of apical tissue including the SAM were dissected from plants expressing either Hd3a, RFT1 or exposed to SDs and their transcriptome was analyzed. To obtain SAMs selectively targeted by Hd3a or RFT1, we exploited an inducible system that activates the transcription of either Hd3a or RFT1 in leaves of transgenic *GVG:Hd3a* and *GVG:RFT1* plants upon dexamethasone treatment (Brambilla *et al.*, 2017) .In this way we could compare gene expression changes at the SAM mediated by either full photoperiodic induction or by Hd3a or RFT1 alone.

MATERIALS AND METHODS

Plant growth conditions, DEX treatments and sampling

The background genotype was the variety Nipponbare for all the experiments. Construction and validation of *GVG:Hd3a* and *GVG:RFT1* transgenic plants has been described in Brambilla et al., 2017,although different transgenic lines behaved similarly, for the present study we chose # 25 for *GVG:Hd3a* and #11 for *GVG:RFT1* as they showed good induction, no basal expression and good

regulation of target genes in the leaves. Plants were grown at 16 hours light (at 28°C during the day/ 24°C during the night) for 8 weeks before being leaf sprayed with 10μM dexamethasone + 0.2% Tween or mock treated. Lower DEX concentrations resulted in uneven induction while higher did not result in higher induction, probably saturating the GVG system. Due to the residual variability of transgene induction in leaves in the selected *GVG:Hd3a* and *GVG:RFT1* lines, similar induction of *Hd3a* and *RFT1* was achieved by spraying *GVG:Hd3a* leaves for 5 consecutive days and *GVG:RFT1* leaves for 2 consecutive days; DEX was sprayed at ZT10, with sampling at ZT0 on the day following the last treatment. For short days induction, all plants were grown under long day conditions for 8 weeks, then half of them were shifted to SD, as described by Galbiati et al., 2016. (Galbiati *et al.*, 2016).

RNA extraction, transcriptomics, GO terms and quantitative RT-PCRs

The transcriptomic analyses were performed in triplicate, with the exception of Hd3aDEX/mock where one sample was discarded because divergent from the other two (see below). To this end, three pools of 4-5 SAM manually dissected with a scalpel under a stereomicroscope were sampled on the day following the last DEX treatment. RNA was extracted using NucleoZOL (Macherey-Nagel) and residual DNA removed using DNase I (Turbo™ DNAse, Invitrogen). Stranded cDNA library was prepared and sequenced with 150 bp paired-end reads (about 35M pairs of reads per sample were obtained) with Illumina HiSeq2500 at IGA, Udine, Italy. Exploratory analyses based on dimensionality reduction of gene expression profiles (MDS-plot) were performed to assess the overall consistency of biological replicates. As outlined in Fig. S1c, one pair of replicates (induced population as well as the control) of the *GVG:Hd3a* experiment formed a distinct, isolated cluster in the multi-dimensional space, suggestive of batch effects. Accordingly, this pair of replicates was discarded from subsequent analyses.

Reads were aligned to the MSU reference of the Os-Nipponbare-Reference-IRGSP-1.0 genome as available from http://rice.uga.edu/, by means of the bowtie2 software; gene expression levels were estimated by RSEM. Differential analyses of gene expression were executed by means of the edgeR; the Genewise Negative Binomial Generalized (glmQLFTest) was applied to test for statistically significant differences. P-values were corrected using the Benjamini Hochberg procedure for the control of the False Discovery Rate. Only genes showing a p-value <= 0.05 following the FDR adjustment were considered to be differentially expressed (DEGs). Data have been uploaded at https://www.ncbi.nlm.nih.gov/geo/query/acc.cgi?acc=GSE226057.

Venn Diagrams in Fig. 2d,e were made with the online tool of the Bioinformatics and Evolutionary Genomics platform. All genes except three (LOC_Os01g59410, LOC_Os07g41410 and

LOC_Os09g09040) and two (LOC_Os05g09500, LOC_Os06g36560) in the intersection between and GVG:RFT1 or GVG:Hd3a respectively and SD in Fig. 2d were differentially expressed in the same direction; these five genes were assigned in the Venn diagram to the change in direction observed under SD. GO terms were searched in the Panther GO-slim Molecular function database, using AMIGO2 (based on panther), p-values are reported in Table S4.

RNA extracted for qRT-PCR analyses was retrotranscribed with ImProm-II™ Reverse Transcriptase (Promega), using 1 µg of total RNA as a starting template and a polyT primer Ubiquitin on Chr6 was used to normalize. Three biological replicas were performed for each sample. Maxima SYBR Green qPCR Master Mix (Thermofisher) was used in a RealPlex2 thermocycler (Eppendorf). All primers used are listed in Table S5.

In situ hybridizations

Nipponbare *wt* meristems were collected in FAA solution (5:5:50:40 formaldehyde, glacial acetic acid, 96% ethanol, water) according to the desired developmental stages (vegetative meristem VM and secondary branches meristem SBM), dehydrated with t-butyl-alcohol, embedded in Paraplast ® and cut in 7µm thick longitudinal sections. Probes (between 150 and 200 bp long, not hydrolyzed) were produced from PCR products (see primers in Table S5) by DIG-RNA labelling kit (Roche) and hybridization was performed at 60°C as described in (Toriba *et al.*, 2019).

Expression and Promoter analysis

Affymetrix microarray expression profiles were retrieved from BAR (http://bar.utoronto.ca/).. Promoters were defined as regions spanning 1100 bp (from –1000 upstream to +100 bp downstream) from the transcription start site (TSS) of the MSU rice gene models; those of DEGs were analyzed by Pscan to identify over-represented position frequency matrices (PFMs), that summarize occurrences of each nucleotide at each position in a set of observed transcription factor-DNA interactions.

PFMs were obtained from the “non-redundant" core collection of plants PFMs as available from the 2020 release of the Jaspar database (https://jaspar.genereg.net/). Only PFMs pscan pValue <0.01 were considered significantly enriched.

CRISPR mutants and rice transformation

Constructs used for CRISPR were described in (Miao *et al.*, 2013; Hu *et al.*, 2016) Guide RNAs (Table S5) were designed using CRISPR-P v2.0, (hzau.edu.cn) in the genes positions as described in Fig. S6a. phenotypic analyses were performed on homozygous T2 plants.

Phylogenetic analysis

BRT1 protein homologues were searched using Blast-P. The 13 closest homologues proteins were retrieved and three homologues were added from *Arabidopsis thaliana.* Protein alignment and guide tree were constructed with CLUSTAL O (1.2.4) online tool.

Tiller angle measurements

Plants were grown for eight weeks under LD then shifted to SD. Tiller angles were measured with ImageJ as described by the widest angle (θ) between the main culm and a culm deriving from it (see θ drawing in Fig.4b).

RESULTS

Inducible overexpression of *Hd3a* or *RFT1* in leaves under LD is sufficient to activate transcription of inflorescence markers at the SAM

Shortening days induce transcription of *Hd3a* and *RFT1* in leaves, their movement through the phloem, and ultimately the switch of SAM development to reproductive growth (Song et al., 2017; Brambilla & Fornara, 2017) Transcription of many genes expressed at the SAM is sensitive to changes in day length but how Hd3a and RFT1 coordinate transcription of target genes is currently unclear (Gómez-Ariza *et al.*, 2019). Florigens are largely redundant as single null mutations (*hda3-1* to *3* and *rft1-1* to *2* - for CRISPR mutants constructions see following paragraph) but the double *hd3a rft1* mutant is never flowering (Fig.1.a,b); nevertheless it is unclear if they are adjuvated by additional factors under short day inductive conditions. Moreover, the contribution of Hd3a and RFT1 to gene expression at the SAM might be unequal, with transcription of some genes depending predominantly on either of the two.

To dissect Hd3a or RFT1 specific functions as transcriptional regulators, we used transgenic lines previously developed and validated in the cultivar Nipponbare that conditionally overexpress either Hd3a (*GVG:Hd3a*) or RFT1 (*GVG:RFT1*) upon dexamethasone (DEX) leaf spray (Brambilla *et al.*, 2017). We assessed the effectiveness of this system to interrogate gene expression changes at the SAM upon *Hd3a* or *RFT1* induction. Plants were grown under LDs to avoid endogenous expression of *Hd3a* or *RFT1* and the expression of the transgene was then induced by dexamethasone leaf spray. We quantified in leaves and SAMs the induction of the transcripts of both *Hd3a* and *RFT1*, as well

as that of markers of inflorescence development. Expression of *Hd3a* and *RFT1* was strongly induced in leaves upon DEX treatment, but no expression was detected in the SAMs (Fig. 1d, e). We previously reported (Brambilla et al., 2017) that DEX induction of *Hd3a* and *RFT1* in leaves could induce *OsMADS14* and *OsMADS15* locally; here we show that transcription of targets of Hd3a and RFT1, including *OsMADS14*, *OsMADS15* and *OsMADS34*/*PANICLE PHYTOMER2* (*PAP2*), was induced in SAMs of DEX-treated but not mock-treated plants, indicating that transgenic Hd3a and RFT1 proteins are normally translocated to the SAM where they are active and can reproduce transcriptional responses typical of exposure to SD (Fig. 1f-h) (Kobayashi et al., 2010; Taoka et al., 2011; Tamaki et al., 2015) . We quantified transcription of marker genes also in apices of 2 months old plants grown under LD and then exposed to 12 SDs, that are sufficient to commit the apex to flowering (Gómez-Ariza *et al.*, 2019). *OsMADS14*, *OsMADS15* and *OsMADS34/PAP2* were more strongly upregulated in SD SAMs compared to the conditions in which only one florigen was expressed (Fig. 1f-h). This difference was expected since 12 SDs allow longer exposure of apical cells to both florigens, and more time to commit the SAM compared to DEX-induction, which is characterized by a shorter exposure and is mediated only by the expression of a single florigen. Notably, *GVG:RFT1* plants treated with DEX could accelerate flowering under LD similarly to plants exposed to SD, whereas *GVG:Hd3a* plants could not (Fig. 1c). These divergent responses could be due to quantitative differences in activation of inflorescence identity genes, failing to reach the threshold necessary for the reproductive switch in *GVG:Hd3a* plants (Fig. 1f-h). Alternatively, Hd3a might require additional factors to induce flowering in a few days, which are missing under LD. We conclude that DEX treatments of *GVG:Hd3a* and *GVG:RFT1* plants recapitulate the major molecular events occurring at the SAM upon exposure to SDs, yet DEX treatment of *GVG:Hd3a* plants was unable to irreversibly commit the SAM to flowering(Gómez-Ariza et al., 2019)(Gómez-Ariza et al., 2019).

Global transcriptional changes occurring at the SAM upon photoperiodic or florigenic induction

To describe the contribution of either Hd3a or RFT1 to global transcriptional changes that occur at the SAM during floral induction, we performed a comparative transcriptomic analysis of DEX treated *vs.* mock-treated *GVG:Hd3a* and *GVG:RFT1* meristems (Fig. 2a, b). We also compared the transcriptome of *wt* SAMs continuously grown under LD or grown under LD and then exposed to 12 consecutive SDs (12 SD) (Fig. 2c) that identify gene expression changes required to commit the SAM to reproductive growth (Gómez-Ariza et al., 2019)(Gómez-Ariza et al., 2019). Comparison between SD and DEX-mediated treatments was necessary to ensure that observed gene expression changes

were in the biological context of flowering commitment.

Meristem sampling and descriptive statistics concerning the total number of reads and of reads assigned to *O. sativa* gene models are reported in Fig. S1a,b.

We found 5221 differentially expressed genes (DEGs) between shoot apices of wild type plants grown under LD and exposed to 12 SDs. Equivalent analyses recovered a total of 1957 and 363 DEGs induced by DEX treatment in *GVG:RFT1* and *GVG:Hd3a*, respectively (Table S1). Interestingly, 903 of the *GVG:RFT1* DEGs and 114 of the *GVG:Hd3a* DEG were recovered in SAM after SD exposure but not in the other transgenic line. A total of 28 genes were regulated by Hd3a and RFT1 but not by photoperiod. Finally, a total of 71 genes were found to be differentially expressed in all the comparisons performed in this study (Fig. 2d, the list of genes resulting from the overlap between datasets is shown in Table S2). These genes are likely to carry out important regulatory functions during the initial phases of floral transition. Gene Ontology (GO) analyses show an enrichment in regulative molecules among the differentially expressed genes across the three datasets and the intersection between them (Fig. S2; Table S4) suggesting the activation of a transcriptional cascade. Although flowering time quantifications (Fig.1c) and the expression level of marker genes suggest a difference in the strength of induction of the three treatments, with the strongest treatment being exposure to 12 SDs, followed by RFT1 and finally by Hd3a induction, a correlation analysis performed on the first 2000 DEG (ordered by padj) suggested that Hd3a and RFT1 regulate the transcriptome following a similar direction (Fig. S1d). Looking at DEGs in the three datasets we observed for example that several auxin signaling factors were differentially expressed in one or more comparison, including *OsIAA2* (*GVG:Hd3a* dataset), *OsIAA 2,3,6,12,13,17,25* (*GVG:RFT1*), *OsIAA2,6,7,13,14,15,24,30* (SD). Also, all four *RICE CENTRORADIALIS* (*RCN)* genes were significantly deregulated in the SD dataset, but only *RCN1* and *RCN4* were differentially expressed in the RFT1 dataset.

To further restrict the number of genes to be considered for downstream analyses and select genes showing stronger de-regulation under our experimental conditions, we applied a stringent filter of $\log_2 FC \geq |1.5|$ (Fig. 2e). A total of 225 DEGs met this condition in the SD dataset, of these, 111 were upregulated and 114 downregulated. Equivalent figures in the *GVG:Hd3a* and *GVG:RFT1* datasets account for 49 genes (33 upregulated and 16 down) and 194 genes (165 up and 29 down) respectively (Fig. 2e) . Interestingly we noticed that, while under SD induction an almost perfect balance between up and downregulated DEGs is observed, in the *GVG:RFT1* and *GVG:Hd3a* datasets upregulated genes were overrepresented .

We therefore described transcriptional changes triggered by natural SD exposure, that includes (but it is not restricted to) the induction of *Hd3a* and *RFT1* expression, and by the induction of *Hd3a* or

RFT1 expression alone under LD conditions, retrieving many common genes but also some differences in the targets and in the strength of their induction.

Common genes differentially expressed at the SAM upon photoperiodic or florigenic induction

By applying the stringent criteria outlined above, we retrieved 15 genes responding to all treatments (Fig. 2e,f). This list includes known florigens targets: *OsMADS14*, *OsMADS15*, *OsMADS18* and *OsMADS34*/*PAP2*, all of which were upregulated, and are known to be essential for proper transition to reproductive growth of the apex (Kobayashi et al., 2012). *OsFT-L1*, a member of the PEBP family, highly similar to *Hd3a* and *RFT1,* was strongly upregulated (Izawa et al., 2002). It is required to potentiate the florigenic effect of Hd3a and RFT1, and to enhance panicle determinacy(Giaume *et al.*, 2023).

Although the *PINE1* transcription factor, a known target of *Hd3a* and *RFT1*, did not show a $\log_2$FC > |1.5| in *GVG:Hd3a* DEX-treated plants, we decided to include it in Fig. 2f, because of its known effect on stem elongation in response to florigenic signals (Gómez-Ariza *et al.*, 2019) .

Thus, out of 16 genes selected by these criteria from the three datasets, 6 were already known to be relevant to the reproductive switch, suggesting that the remaining uncharacterized genes might be good candidates contributing to this process. Of note among these 16 genes, only *PINE1* and *LOC_Os01g04750*, that encodes for an AP2-B3 containing transcription factor, were down regulated by the florigens and SDs (Fig. 2f).

Among the 10 genes not previously associated with the reproductive switch, 5 belonged to diverse classes of regulatory proteins, 3 were related to transposable elements and 2 were uncharacterized proteins without known conserved domains. Regulatory proteins included a MATE efflux carrier (a proton-dependent efflux transporter), a small hydrophylic Late Embryogenesis Abundant (LEA) protein, the Auxin-responsive Aux/IAAprotein OsIAA2, the F-box domain containing protein OsFBX125, that we renamed BROADER TILLER ANGLE 1 (BRT1) after its functional characterization, and *LOC_Os01g04750* encoding for a transcription factor containing both AP2/ERF and B3 domains. Genes annotated as transposable elements (TE) included *LOC_Os04g29310, LOC_Os08g13680* and *LOC_Os07g32406*. Similarity search with the *LOC_Os07g32406* coding sequence among plant expressed genes, showed that it contains a derived plant mobile domain (PMD) that is present in a class of proteins involved in TE silencing, genome stability, and in the control of cell differentiation and meristem maintenance. It is similar to MAINTENANCE OF MERISTEM LIKE 1 (MAIL1) of Arabidopsis (Ühlken *et al.*, 2014; Ikeda *et al.*, 2017; Nicolau *et al.*, 2020). Therefore, we renamed *LOC_Os07g32406* as *OsMAIL1.* According to the microarray expression profiles collected in the Bio-Analytic Resource Database (BAR), *OsIAA2* is expressed through the

entire life of the plant, except for the late reproductive and embryo/endosperm tissues, *OsMAIL1* is highly expressed in the stigma and in the ovary; *BRT1* is found in all reproductive stages and tissues, peaking in younger inflorescences and ovary, *MATE* is expressed in all plant tissues, with a preference for young leaves and mature seeds and LOC_Os01g04750, the B3/AP2 TF, besides the SAM can be found in young seedlings. As expected, all genes are expressed in the SAM but also none of them is restricted to it, suggesting that their role is not limited to floral commitment (Fig. S4a).

Promoter analysis was performed to characterize common regulatory patterns in Hd3a, RFT1 or SDs DEGs to identify -if any- enrichment of specific transcription factor binding sites (TFBS). For every set of DEGs, up- and down- regulated genes were analyzed separately. Only TFBS associated with a p-value<0.01 according to pscan were considered enriched. Interestingly, a specific pattern of enrichment was associated with each set of DEGs, suggesting that florigens control gene expression by exploiting different cis elements syntaxes. SD and RFT1 datasets seem to share a high similarity in the represented TF families, both for up and down-regulated gene sets (Fig. S4b). In the first case, the most present are bHLH and tryptophan cluster factors (to whom the MYB subclass belongs), while in the latter the most present are A.T. hook and B3 factors. On the other hand, Hd3a datasets show a different enrichment in both subsets (Fig. S4b). Promoters of up-regulated genes seem to be enriched mainly with bHLH binding sites (although in a very different proportion than SD and RFT1 datasets), while promoters of down-regulated genes appear to be targets of bZIPs. Hd3a shows generally fewer DEGs than the other datasets. To define the spatial distribution of transcripts during floral commitment for *OsIAA2*, *OsMAIL1* and *MATE* we performed *in situ* hybridizations using probes on apical meristems at vegetative (VM) and secondary branch meristems (SBM) stages (Fig. S3). *OsMAIL1* transcripts were almost absent from the VM while were detected at advanced developmental stages in both SBM as well as spikelet meristem (SM) stages. *MATE* and *OsIAA2* transcripts were detected already at the VM stage in the SAM and in young leaf primordia. At later developmental stages, transcripts were localized in SBM and floret meristem (FM). These data indicate that *OsIAA2*, *OsMAIL1* and *MATE* are transcribed during the floral transition.

Expression analysis of florigen targets in *hd3a, rft1* and *hd3a rft1* double mutants

The RNA-seq analyses identified genes whose transcription responds to Hd3a and RFT1 at the apex, showing that several targets are differentially sensitive to florigens induction. To verify that Hd3a and RFT1 are not only sufficient but also necessary for transcriptional regulation of the target genes, we generated *hd3a* and *rft1* single (Fig. S5a) as well as *hd3a rft1* double mutants and assessed expression of some targets in these genotypes. Six frameshift mutant alleles were obtained for *hd3a* and two for *rft1* (Fig. S5c,d) and also, an in-frame 6bp deletion in *RFT1*.

As expected, under SD all homozygous *hd3a* CRISPR mutants flowered later than the wild type (Fig. 1a) while no significant delay in flowering was observed in *rft1* mutants. All *rft1* knock-out mutants were late flowering under LD, while no alteration in flowering was observed in the -6bp in frame *rft1-3* mutant, suggesting that the two aminoacids deletion does not affect RFT1 protein function.

We crossed *hd3a-4* and *rft1-1* (Fig. S5c,d), and we obtained a new double biallelic mutant containing *hd3a-4* and the novel *hd3a-7* allele carrying a -15 bp deletion and *rft1-1 rft1-2* mutations. This *hd3a rft1* double mutant is unable to flower under any photoperiod (Fig. 1a,b), suggesting that, unlike the two aminoacids missing in *rft1-3* allele, the five amino acids missing in *hd3a-7* are important for Hd3a function.

Expression levels of the 10 DEGs common to SD, Hd3a and RFT1 and showing a marked change in their expression levels were measured in SAMs obtained from *hd3a-2, hd3a-3* and *rft1-1* single frameshift mutants and the *hd3a rft1* double mutant, under LD and after exposure to inductive SDs. Concomitantly, we also assayed the expression of the four *RCN*s as all four were significantly deregulated in the SD dataset, and *RCN1* and *RCN4* were also differentially expressed in the RFT1 dataset. Relative expression levels (*hd3a*, *rft1* or *hd3a rft1* mutants *vs wt*) of these genes in SAMs exposed to 12 SDs for single mutants or 15 SDs for double mutants are reported in Fig. 3a,b These fall below 1 for all genes analyzed confirming a dependency on the florigens for their expression at 12/15 SD, except for *LOC_Os01g04750* that is downregulated in the RNA-seq datasets and accordingly is more expressed in the florigens mutants compared to the *wt*. The complete time course during floral commitment was also analyzed and supports this observation (Fig. S6). Interestingly, although Hd3a is the major contributor to floral commitment in SD conditions (Fig. 1a), the expression of the selected target genes appears to be more affected in *rft1* mutant plants rather than *hd3a* (Fig. 3a, Fig. S6). As expected, a more marked decrease in relative expression levels is observed in *hd3a rft1* double mutants on average, suggesting an additive effect of the florigens. Notably, we observed that both *OsIAA2* and *MATE* expression levels were only slightly affected in all mutants, (Fig. 3a, Fig. S6) suggesting that Hd3 and RFT1 are sufficient but are not necessary to activate *OsIAA2* and *MATE* transcription, and other regulators might be involved for these genes.

Dependency on florigens expression, and especially on RFT1, was also confirmed for all 4 RCNs, pointing out the dependency of antflorigens expression on florigens in rice (Fig. 3b).

Mutation of the photoperiod and florigen targets *LOC_Os01g04750*, *OsMAIL1* and *BRT1* did not affect heading date

We used the CRISPR/Cas9 system to obtain single knock out mutants of 3 of the 10 differentially expressed genes (Fig. 2e). We selected the F-box containing *BRT1/OsFBX125* gene,

LOC_Os01g04750, that was the only downregulated gene, and *OsMAIL1*; on their sequences we designed specific guide RNAs (Fig. S7a-c).

F-box proteins are important developmental regulators as they target proteins for degradation by the proteasome and many of them have been already described to be involved in various developmental processes including flowering (Ikeda *et al.*, 2007; Ikeda-Kawakatsu *et al.*, 2009; Fornara *et al.*, 2009; Song *et al.*, 2012). In rice there are more than 850 F-box proteins with different types of domain organization (Xu *et al.*, 2009). BRT1 contains an F-box in the N-terminal part, Leucin Rich Repeats (LRR) in the middle of the protein and an F-box Associated Domain (FBA) at the C-Terminal. This domain organization is found in many F-box proteins throughout the plant kingdom. Although many F-box containing proteins were differentially expressed in the three datasets, only *BRT1/OsFBX125* was strongly upregulated in all of them. *OsMAIL1* was chosen because of its similarity to Arabidopsis *MAIL1,* a gene that determines cell differentiation and meristem maintenance.

For *LOC_Os01G04750* and *OsMAIL1,* knock out mutants with a frame shift close to the ATG were obtained, while, for *BRT1* we directed the gRNA to two different regions of the gene generating two sets of mutants (Fig. S7a-d): those harboring frame shift mutations introducing a premature stop codon close to the ATG (null mutants) and those with a premature stop codon close to the FBA (ΔC mutants). Putative protein products (Fig. S7e) are likely to be present as their mRNA is expressed similarly as in the *wt* (Fig. S7f).

When flowering time of independent mutants in all three genes was analyzed under SD, no difference compared to Nipponbare *wt* was observed, suggesting that these genes might either control flowering redundantly with other factors or they are involved in aspects of the flowering transition other than timing (Fig. 4a).

BROADER TILLER ANGLE 1 (BRT1) is an F-box protein that controls tiller angle and spikelet development

Search for proteins similar to BRT1 showed that its closest homologous are retrieved in different species belonging to the *Poacee* family (Fig 4i, Fig.S8), suggesting that, while no *BRT1* homologous are present in rice genome, this it is quite conserved in different species. Proteins with high degree of similarity are also present in *Arabidopsis thaliana*, where BRT1 closest relative is At1g69630. Transcriptional analysis showed that *BRT1* is mildly expressed in vegetative tissues, and it is induced at the SAM by the switch to reproductive development (Fig. S6); then it is predominantly expressed in the inflorescence and in the ovary (Fig. S4a).

When we analyzed *brt1* mutant plants, we observed that some mutant alleles showed a broader tiller angle between the main culm and the first tillers to form, as well as between the first tillers and those

that arise later (Fig. 4b). We measured the angle (ϑ) between the main culm and the outermost tiller in ΔC mutant alleles *brt1-2*, *brt1-3, brt1-5* and *brt1-7* and in null mutants *brt1-c* and *brt1-e* grown under LDs for 8 weeks and then shifted to SD conditions (Fig. 4b). In the ΔC mutants *brt1-5* and *brt1-7* and in both null mutants analyzed, we observed a broader tiller angle compared to the *wt* (Fig. 4e). In ΔC mutants the angle was already different under LD conditions (vegetative growth) and the difference persisted after floral commitment under SD. In null mutants the broader tiller angle was particularly visible only after commitment. As not all ΔC mutants showed a broader tiller angle compared to the *wt*, we supposed that some could still express a largely functional BRT protein. We then checked *BRT1* expression in the vegetative SAM (grown under LD) and in the SAM committed to flowering (exposed to 12 SD) in *brt1-2* (as an example of the allele which does not show differences from the *wt* in tiller angle) and *brt1-7* (representative of the allele showing wider tiller angle than the *wt*) and we observed no relevant expression differences with the *wt*, suggesting that the transcript is present and likely functional in *brt1-2*, while is the peculiar C-terminal protein sequence formed in *brt1-7* and possibly *brt1-5* that causes an exacerbated defect in tiller angle (Fig. S7e).

A more detailed inspection of the panicles in the two null mutants *brt1-c* and *brt1-e* showed additional defects in inflorescence development: we observed one or two bracts, with variable length, developing form the basal node of the panicle (Fig. 4c-arrow), and the development of the sterile glumes that reach a length that surrounds the glume (Fig. 4d). Such characteristics, very rarely present in *wt* plants, are very frequent in *brt1* null mutants. (Fig. 4f,g,h).

Fare clic o toccare qui per immettere il testo.

DISCUSSION

Flowering in rice depends on Hd3a and RFT1. They act as long-distance systemic signals produced in leaves upon perception of favorable photoperiods and acting at the SAM to reprogram gene expression. Although Hd3a and RFT1 are largely redundant in the control of flowering, they also have separable functions which have been attributed to their distinct transcriptional regulation in the leaves (Komiya *et al.*, 2009; Sun *et al.*, 2012). A question that remains open is whether their specific functions could also depend upon differential activities at the SAM. Florigens are regulating gene expression by forming FACs, and part of their diversity resides in the capacity to contact different protein partners, which could account for Hd3a and RFT1 distinct activities, to be interpreted at the post-transcriptional level (Jang et al., 2017; Brambilla et al., 2017; Cerise et al., 2021). We addressed these features of the flowering network, and we also searched for previously unknown florigens targets, by comparing the SAM transcriptomes upon leaf expression of 1) only Hd3a, 2) only RFT1 or 3) both, induced under natural photoperiodic conditions.

Interpretation of global transcriptional changes suggests similar effects of the florigens

The comparison of global transcriptional changes at the SAM seemed to indicate that subsets of genes exist responding preferentially to Hd3a or RFT1: some target genes were differentially expressed only by specific treatments. However, data must be interpreted against the statistical thresholds used in the analysis. Genes falling outside groups characterized by shared treatments often occupied that position because of quantitative and not qualitative features. E.g. when comparing genes from the *GVG:Hd3a* and *GVG:RFT1* datasets we generally observed expression changing in the same direction for a large group of genes, many of which, however, did not meet the statistical thresholds that would place them in a shared group. This was not the case for the SD dataset that identified several genes unique to photoperiodic induction. This suggests that, although florigens alone can trigger expression changes also under non inductive conditions, changes in day length have more pervasive effects than the florigens alone. However, it should be noted that tissues of the SD samples were grown for 12 days under inductive conditions (*GVG:Hd3*a and *GVG:RFT1* were induced by spraying for only 5 and 2 days respectively), likely exposing transcriptional changes that occurred during a more prolonged time, possibly indirect and that could not be captured by DEX-treated samples.

These observations support the conclusions that (i) the two florigens ultimately activate a broad common set of genes and that (ii) differentially expressed genes common to all three datasets are strongly significant as a core set central to floral induction.

Among these genes, we found all those required for panicle development, like *OsMADS14/15/18* and *OsMADS34*/*PAP2.* Quadruple *osmads14*/*15*/*18*/*34* mutants prevent formation of inflorescence branches and spikelets which are replaced by vegetative shoots. Yet, conversion of the VM to IM occurs normally, as indicated by the change in phyllotaxis associated to reproductive development, suggesting other genes might control it (Kobayashi et al., 2012). A plausible candidate for such function, identified within the core set and strongly induced by all treatments, is the florigen-like PEBP OsFT-L1. Its overexpression leads to very precocious flowering without vegetative phase (Izawa *et al.*, 2002). Conversely, *ft-l1* mutants delay flowering and the VM-to-IM transition (Giaume *et al.*, 2023).

The other candidate of known function in the list is the C2H2 transcription factor PINE1, which prevents internode elongation during the vegetative phase. Translocation of Hd3a and RFT1 to the shoot apex reduces *PINE1* transcription and increases stem sensitivity to gibberellins, initiating stem elongation at the same time as the floral transition (Gómez-Ariza *et al.*, 2019).

Among the newly identified genes we have found three proteins putatively involved in DNA metabolism: two helicase-related proteins (LOC_Os04g29310 and LOC_Os08g13680) and a protein similar to Arabidopsis MAIL1 (Ühlken *et al.*, 2014). Helicases bind and unwind DNA while AtMAIL1 was shown to be responsible for silencing transposable elements (TE), that is important to improve genome stability as it avoids the expression of undesired transcripts originated by insertion of TE. Genome stability seems therefore to be an important matter during floral transition, possibly protecting DNA during major transcriptional changes. Differently from previous reports, we did not find many TE, rather more genes with regulatory function (Tamaki et al., 2015). Indeed, at least 8 out of the 16 genes have transcription factor activity, including two of still unknown function: *OsIAA2* and the AP2/B3 domains-containing *LOC_Os01g04750*. We could explain this difference from the different experimental setups: we compared *wt* plants induced and not induced to flowering by SD treatment and plants not expressing and overexpressing the florigens, while Tamaki et al., compared *wt* plants to double *hd3a rft1* RNAi lines; while our three datasets had many common genes, very few, and only *OsMADS15* among the known regulators, were in common with Tamaki's dataset.
Finally, regulation not only include DNA stability and transcription but also proteins turnover, as BRT1 is an F-box protein controlling protein target lifetime by their ubiquitination and sending to proteasome-mediated degradation, and other more specific mechanisms like that controlled by MATE membrane protein efflux carrier.

BRT1 links floral induction and tiller angle

The editing of *LOC_Os01g04750*, *BRT1* and *OsMAIL1* led to mutant plants with the same heading date as the *wt*, indicating that such genes are not directly involved in timing the transition to reproductive growth. However, literature already indicates that florigen function is not limited to flowering time control but involves a suite of traits associated to it. For example, it has been demonstrated that the florigens can synchronize stem elongation with heading (Gómez-Ariza *et al.*, 2019), and Hd3a can form FACs promoting tillering (Tsuji et al., 2015). Therefore, it was not unexpected that phenotypes associated to mutations in core genes responding to florigenic induction could reveal novel links between reproductive commitment and other traits.

During initial rice development, tiller angle widens, during a so-called 'early spread stage' (Yu *et al.*, 2007). This behaviour is believed to allow the young seedlings to better occupy space. Subsequently, during a stage called 'late compact', the tiller angle decreases, reaching a minimum during flowering, possibly to reduce the impact of shading; indeed, erect rice plants are also considered positively in agriculture. The shortening of day length induces the reduction in tiller angle, indicating that the photoperiod has an influence on the trait during the switch to reproductive development (Ouyang *et*

al., 2009). Thus, BRT1 might be the link between photoperiodic flowering and the control of tiller angle.

We isolated two sets of *brt1* mutants: ΔC and null. In all null mutants analysed, the plants cannot reduce the tiller angle under SD, resulting in wider angles at heading. Differently, only two independent ΔC mutant alleles (*brt-5* and *brt-7*) strongly increased tiller angle in a day length-independent manner, showing already wider tiller angles under LD. The more severe phenotype observed in *brt-5* and *brt-7* could be ascribed to the fact that their BRT1 mutant proteins contain similar aminoacidic sequences at the C-term before the stop codon (Fig. S7e, yellow boxes) and these could more dramatically interfere with the mechanism in which BRT1 is involved. We cannot nevertheless exclude that *brt-5* and *brt-7* ΔC mutations create dominant-negative or even gain of function alleles, as we did not obtain heterozygous or biallelic plants that we could test.

As BRT-1 is an F-box protein targeting other proteins to proteasome, we could speculate about the existence of one or more proteins that increase tiller angle under vegetative growth and are targeted to be degraded by BRT1 under SD to establish the 'late compact' phase. As the determination of tiller angle depends upon the shoot gravitropic response and this is linked to the asymmetric distribution of auxin in the shoot, (Wang *et al.*, 2022) BRT1 could be part of a network involving also OsIAA2 integrating gravity perception and auxin signalling. The link between BRT1 and auxin distribution and/or signalling is also corroborated by the observation that in *brt1* null mutants bract growth at the basal node of the rachis is derepressed and sterile glumes develop at the base of the floret, much more frequently than it occurs normally in the wt.

BRT1 is a target of Hd3a and RFT1. Interestingly Hd3a RNAi and overexpressor lines reduced and increased tiller number respectively (Tsuji et al., 2015), but we observed that neither *hd3a* nor *rft1* single mutants could modify tiller angle. This could suggest full redundancy between florigens, which is confirmed by the observation that only a double *hd3a rft1* mutant prevents the increase of *BRT1* transcription at the SAM and it also suggests that RFT1, similarly to Hd3a, can be translocated to axillary meristems, where tiller angle is determined during development. All such hypotheses will need experimental validation.

Aknowledgements

We thank Elisabetta Sergi for helping with the production and characterization of *OsMAIL1* mutants. This work was supported by core funding from the Department of Agricultural and Environmental Sciences of the University of Milan to VB.

FIGURE LEGENDS

Figure 1. Hd3a and RFT1 are required to induce flowering and, when overexpressed in leaves of *GVG:Hd3a* and *GVG:RFT1* plants, activate inflorescence markers at the SAM .

Days to heading under both long day (LD) and short day (SD) of Nipponbare *wt*, *hd3a* and *rft1* mutants, as well as double mutant *hd3a rft1* (a). Red dotted line represents the flowering time of the *wt* in SD conditions, blue dotted line the flowering time of the *wt* in LD conditions while black dotted line indicates the never flowering (NF) phenotype of the double *hd3a rft1* mutant, after exposure to 200+ short days. Same age plants (grown for 2 months under LD and then for 2 months under SD conditions) of *hd3a, rft1* and *hd3a rft1* double mutant: only the latter is unable to flower (b). In (c) days to heading counted from beginning of DEX treatment or SD exposure of treated (DEX and SD) and untreated samples (mock and LD). Expression levels of *Hd3a* in leaves and SAM of *GVG:Hd3a* plants (d) and *RFT1* in leaves and SAM of *GVG:RFT1* plants (e) after treatment with dexamethasone (DEX). Expression levels of *OsMADS14* (f), *OsMADS15* (g) and *OsMADS34* (h) in non-inductive (mock and LD) and inductive (DEX treated and SD) conditions at the SAM of *GVG:Hd3a*, *GVG:RFT1*, and wt plants. Expression levels have been normalized on ubiquitin. Error bars (a,b,c,d,e,f) represent standard deviations. T tests were conducted on inductive conditions *vs* non-inductive and *=padj<0.5, **=padj<0.01, ***=padj<0.001, ****=padj<0.0001.

Figure 2. Transcriptomic analyses of SAMs during single florigenic or full photoperiodic induction.

RNA-seq experimental setup: *GVG:Hd3a* (a), *GVG:RFT1* (b) and *Nipponbare* (c) SAMs were sampled (dashed circle) before and after florigens and other signals from leaves move to the SAM (arrow indicates movement). In (d-e): Venn diagram showing numbers of genes differentially expressed in each dataset and overlaps between differentially expressed genes among the three datasets; (d): all genes, No FC trimming was applied, padj>0.05, in (e): genes were filtered at p<0.05 and $\log_2$FC > |1.5|. Genes up- and downregulated compared to controls are indicated with red and blue arrows. **PINE,* listed in (f), here is omitted. (f): list of the 15 differentially expressed genes at the overlap between *GVG:Hd3a*, *GVG:RFT1* and SD induction. Red: genes upregulated; blue: genes downregulated. *PINE1* was added to the list even if its $\log_2$FC falls just below 1.5 in *GVG:Hd3a* plants.

Figure 3. Flowering time of florigen mutants and their targets expression

Ratios between the expressions under flowering inducing conditions (12SDs for single mutants and 15SDs for double mutants) of the 10 uncharacterized genes retrieved from the crossed RNA-seq datasets (a), and of RCNs (b) in single (*hd3a* (red) and *rft1* (blue)) and double mutants (*hd3a rft1*(purple)) *vs* the expression in the *wt.* 2 biological replicas × 3 three technical replicas each were

used. Error bars represent standard deviations. T tests were conducted on mutated *vs wt* backgrounds: *=padj<0.5, **=padj<0.01, ***=padj<0.001, ****=padj<0.0001.

Figure 4. Phenotypes of gene edited plants in *BRT1*, *OsMAIL1* and *LOC_Os01g04750* and phylogenetic relationship of BRT1 homologous among different species

Days to heading (a) of edited alleles of *BRT1* (*brt1-2,-3,-5,-7* and *brt1-c,-e*), *OsMAIL1* (*mail1-1, mail1-2, mail1-3, mail1-4, mail1-5*) and *LOC_OS01G04750* (*loc_os01g04750 -1, loc_os01g04750 -2, loc_os01g04750 -4*) grown under continuous SD. Error bars represent standard deviations. There was no statistically significant difference between any of these mutant lines and the *wt*. Additional phenotypes observed in *brt1* mutants are shown in (b-g). In (b) tiller angle (ϑ, measured as the angle between the main culm and the outermost tiller) of ΔC mutant allele *brt1-7* compared to the *wt* and in (e) tiller angle ϑ measured in *brt1-5* and *brt1-7* ΔC (yellow) and *brt1-c* and *brt1-e* null (purple) mutants compared to the *wt* (black) in plants grown under LD. The line represents the average measurement and the shade the standard deviation. In (c) white arrows pointing at the unsuppressed basal bract and in (d) the abnormally developed sterile glume in *brt-e* null mutant compared to the *wt*. Scale bars are 10mm (c) and 1mm (d). In (f) percentage of plants showing at least one basal node bract and one extra glume and in (g) the average percentage of extra glumes per panicle in *wt* plants and (h) *brt-null* plants. (i) Guide tree of BRT1 homologues found in *Poacea*e species and in Arabidopsis; species name and protein ID is specified; scores correspond to distance measures. T tests were conducted as mutated backgrounds *vs wt* and *=padj<0.5, **=padj<0.01, ***=padj<0.001, ****=padj<0.0001.

SUPPORTING INFORMATION

Fig. S1. Meristem sampling, RNA-seq descriptive statistics, consistency of biological replicates and correlation between DEG in *GVG:Hd3a* and *GVG:RFT1*.
Fig. S2 GO terms of all DEG in SD, *GVG:Hd3a*, *GVG:RFT1* and the CROSS between them.
Fig. S3 Expression patterns of *OsIAA2*, *OsMAIL1* and *MATE* at the SAM
Fig. S4. Global expression profiles of 10 uncharacterized genes and TFBS enrichment in the promoters of the RNA-seq-retrieved genes
Fig. S5. Gene structure of the florigens and CRISPR-edited alleles
Fig. S6. Time course of the expression levels of the ten uncharacterized genes in single and double mutants in the florigens
Fig. S7. Gene structures of the *BRT1, OsMAIL1* and *LOC_Os01g04750* and CRISPR mutant alleles retrieved
Fig. S8. Multiple protein alignment of BRT1 with its closest homologues from other *Poaceae* species and with Arabidopsis

Supplementary tables (submitted separately)

Table S1 Differentially expressed genes (SD or dex induced *vs* not induced) in single datasets

Table S2 Differentially expressed genes across multiple datasets

Table S3 Differentially expressed genes across multiple datasets

Table S4 GO terms statistics

Table S5 Primers list

REFERENCES

Ahn JH, Miller D, Winter VJ, Banfield MJ, Lee JH, Yoo SY, Henz SR, Brady RL, Weigel D. **2006**. A divergent external loop confers antagonistic activity on floral regulators FT and TFL1. *The EMBO Journal* **25**: 605.

Baumann K, Venail J, Berbel A, Domenech MJ, Money T, Conti L, Hanzawa Y, Madueno F, Bradley D. **2015**. Changing the spatial pattern of TFL1 expression reveals its key role in the shoot meristem in controlling Arabidopsis flowering architecture. *Journal of Experimental Botany* **66**: 4769–4780.

Bradley D, Carpenter R, Copsey L, Vincent C, Rothstein S, Coen E. **1996**. Control of inflorescence architecture in Antirrhinum. *Nature* **379**: 791–797.

Brambilla V, Fornara F. **2017**. Y flowering? Regulation and activity of CONSTANS and CCT-domain proteins in Arabidopsis and crop species. *Biochimica et Biophysica Acta - Gene Regulatory Mechanisms* **1860**: 655–660.

Brambilla V, Martignago D, Goretti D, Cerise M, Somssich M, De Rosa M, Galbiati F, Shrestha R, Lazzaro F, Simon R, *et al.* 2017. Antagonistic transcription factor complexes modulate the floral transition in rice. *Plant Cell* **29**: 2801–2816.

Cerise M, Giaume F, Galli M, Khahani B, Lucas J, Podico F, Tavakol E, Parcy F, Gallavotti A, Brambilla V, *et al.* 2021. OsFD4 promotes the rice floral transition via florigen activation complex formation in the shoot apical meristem. *New Phytologist* **229**: 429–443.

Chen Q, Payyavula RS, Chen L, Zhang J, Zhang C, Turgeon R. **2018**. FLOWERING LOCUS T mRNA is synthesized in specialized companion cells in Arabidopsis and Maryland Mammoth tobacco leaf veins. *Proceedings of the National Academy of Sciences of the United States of America* **115**.

Conti L, Bradley D. **2007**. TERMINAL FLOWER1 is a mobile signal controlling Arabidopsis architecture. *Plant Cell* **19**: 767–778.

Corbesier L, Vincent C, Jang S, Fornara F, Fan Q, Searle I, Giakountis A, Farrona S, Gissot L, Turnbull C, *et al.* 2007. FT protein movement contributes to long-distance signaling in floral induction of Arabidopsis. *Science (New York, N.Y.)* **316**: 1030–3.

Fornara F, Panigrahi KCS, Gissot L, Sauerbrunn N, Rühl M, Jarillo JA, Coupland G. **2009**. Arabidopsis DOF Transcription Factors Act Redundantly to Reduce CONSTANS Expression and Are Essential for a Photoperiodic Flowering Response. *Developmental Cell* **17**: 75–86.

Furutani I, Sukegawa S, Kyozuka J. **2006**. Genome-wide analysis of spatial and temporal gene expression in rice panicle development. *Plant Journal* **46**: 503–511.

Galbiati F, Chiozzotto R, Locatelli F, Spada A, Genga A, Fornara F. **2016**. Hd3a, RFT1 and Ehd1 integrate photoperiodic and drought stress signals to delay the floral transition in rice. *Plant, cell & environment*.

Giaume F, Bono GA, Martignago D, Miao Y, Vicentini G, Toriba T, Wang R, Kong D, Cerise M, Chirivì D, *et al.* 2023. Two florigens and a florigen-like protein form a triple regulatory module at the shoot apical meristem to promote reproductive transitions in rice. *Nature Plants* **9**: 525–534.

Gómez-Ariza J, Brambilla V, Vicentini G, Landini M, Cerise M, Carrera E, Shrestha R, Chiozzotto R, Galbiati F, Caporali E, *et al.* 2019. A transcription factor coordinating internode elongation and photoperiodic signals in rice. *Nature Plants* **5**: 358–362.

Hu X, Wang C, Fu Y, Liu Q, Jiao X, Wang K. **2016**. Expanding the Range of CRISPR/Cas9 Genome Editing in Rice. *Molecular Plant*.
Huang NC, Jane WN, Chen J, Yu TS. **2012**. Arabidopsis thaliana CENTRORADIALIS homologue (ATC) acts systemically to inhibit floral initiation in Arabidopsis. *Plant Journal* **72**: 175–184.
Ikeda K, Ito M, Nagasawa N, Kyozuka J, Nagato Y. **2007**. Rice ABERRANT PANICLE ORGANIZATION 1, encoding an F-box protein, regulates meristem fate. *Plant Journal* **51**: 1030–1040.
Ikeda Y, Pélissier T, Bourguet P, Becker C, Pouch-Pélissier MN, Pogorelcnik R, Weingartner M, Weigel D, Deragon JM, Mathieu O. **2017**. Arabidopsis proteins with a transposon-related domain act in gene silencing. *Nature Communications* **8**: 1–10.
Ikeda-Kawakatsu K, Yasuno N, Oikawa T, Iida S, Nagato Y, Maekawa M, Kyozuka J. **2009**. Expression level of ABERRANT PANICLE ORGANIZATION1 determines rice inflorescence form through control of cell proliferation in the meristem. *Plant Physiology* **150**: 736–747.
Izawa T, Oikawa T, Sugiyama N, Tanisaka T, Yano M, Shimamoto K. **2002**. Phytochrome mediates the external light signal to repress FT orthologs in photoperiodic flowering of rice. *Genes and Development* **16**: 2006–2020.
Jang S, Li H-Y, Kuo M-L. **2017**. Ectopic expression of Arabidopsis FD and FD PARALOGUE in rice results in dwarfism with size reduction of spikelets.
Kaneko-Suzuki M, Kurihara-Ishikawa R, Okushita-Terakawa C, Kojima C, Nagano-Fujiwara M, Ohki I, Tsuji H, Shimamoto K, Taoka KI. **2018**. TFL1-Like Proteins in Rice Antagonize Rice FT-Like Protein in Inflorescence Development by Competition for Complex Formation with 14-3-3 and FD. *Plant and Cell Physiology*.
Karlgren A, Gyllenstrand N, Källman T, Sundström JF, Moore D, Lascoux M, Lagercrantz U. **2011**. Evolution of the PEBP gene family in plants: functional diversification in seed plant evolution. *Plant physiology* **156**: 1967–1977.
Kaur A, Nijhawan A, Yadav M, Khurana JP. **2021**. OsbZIP62/OsFD7, a functional ortholog of FLOWERING LOCUS D, regulates floral transition and panicle development in rice. *Journal of Experimental Botany* **72**: 7826–7845.
Kobayashi K, Maekawa M, Miyao A, Hirochika H, Kyozuka J. **2010**. PANICLE PHYTOMER2 (PAP2), encoding a SEPALLATA subfamily MADS-box protein, positively controls spikelet meristem identity in rice. *Plant and Cell Physiology* **51**: 47–57.
Kobayashi K, Yasuno N, Sato Y, Yoda M, Yamazaki R, Kimizu M, Yoshida H, Nagamura Y, Kyozuka J. **2012**. Inflorescence meristem identity in rice is specified by overlapping functions of three AP1/FUL-like MADS box genes and PAP2, a SEPALLATA MADS box gene. *The Plant cell* **24**: 1848–59.
Kobayashi K, Yasuno N, Sato Y, Yoda M, Yamazaki R, Kimizu M, Yoshida H, Nagamura Y, Kojima S, Takahashi Y, Kobayashi Y, Monna L, Sasaki T, Araki T, Yano M. **2002**. Hd3a, a Rice Ortholog of the Arabidopsis FT Gene, Promotes Transition to Flowering Downstream of Hd1 under Short-Day Conditions. *Plant and Cell Physiology* **43**: 1096–1105.
Komiya R, Ikegami A, Tamaki S, Yokoi S, Shimamoto K. **2008**. Hd3a and RFT1 are essential for flowering in rice. *Development* **135**: 767–774.
Komiya R, Yokoi S, Shimamoto K. **2009**. A gene network for long-day flowering activates RFT1 encoding a mobile flowering signal in rice. *Development* **136**: 3443–3450.
Lee C, Kim SJ, Jin S, Susila H, Youn G, Nasim Z, Alavilli H, Chung KS, Yoo SJ, Ahn JH. **2019**. Genetic interactions reveal the antagonistic roles of FT/TSF and TFL1 in the determination of inflorescence meristem identity in Arabidopsis. *Plant Journal* **99**: 452–464.
Liu B, Liu Y, Wang B, Luo Q, Shi J, Gan J, Shen WH, Yu Y, Dong A. **2019**. The transcription factor OsSUF4 interacts with SDG725 in promoting H3K36me3 establishment. *Nature Communications* **10**: 1–14.

Miao J, Guo D, Zhang J, Huang Q, Qin G, Zhang X, Wan J, Gu H, Qu L-J. **2013**. Targeted mutagenesis in rice using CRISPR-Cas system. *Cell research* **23**: 1233–6.
Nakagawa M, Shimamoto K, Kyozuka J. **2002**. Overexpression of RCN1 and RCN2, rice Terminal Flower 1/Centroradialis homologs, confers delay of phase transition and altered panicle morphology in rice. *Plant Journal* **29**: 743–750.
Nicolau M, Picault N, Descombin J, Jami-Alahmadi Y, Feng S, Bucher E, Jacobsen SE, Deragon JM, Wohlschlegel J, Moissiard G. **2020**. The plant mobile domain proteins MAIN and MAIL1 interact with the phosphatase PP7L to regulate gene expression and silence transposable elements in Arabidopsis thaliana. *PLoS Genetics* **16**: e1008324.
Ouyang YN, Li CS, Zhang SQ, Wang HM, Zhu LF, Yu SM, Jin QY, Zhang GP. **2009**. Dynamic changes of rice (Oryza Sativa L.) tiller angle under effects of photoperiod and effective accumulated temperature. *Chinese Journal of Applied Ecology* **20**.
Peng Q, Zhu C, Liu T, Zhang S, Feng S, Wu C. **2021**. Phosphorylation of OsFD1 by OsCIPK3 promotes the formation of RFT1-containing florigen activation complex for long-day flowering in rice. *Molecular Plant* **14**: 1135–1148.
Shrestha R, Gómez-Ariza J, Brambilla V, Fornara F. **2014**. Molecular control of seasonal flowering in rice, arabidopsis and temperate cereals. *Annals of botany* **114**: 1445–58.
Song YH, Smith RW, To BJ, Millar AJ, Imaizumi T. **2012**. FKF1 conveys timing information for CONSTANS stabilization in photoperiodic flowering. *Science* **336**: 1045–1049.
Song S, Y C, L L, Y W, S B, X Z, ZW T, C M, Y G, H Y. **2017**. OsFTIP1-Mediated Regulation of Florigen Transport in Rice Is Negatively Regulated by the Ubiquitin-Like Domain Kinase OsUbDKγ4. *The Plant cell* **29**: 491–507.
Sun C, Fang J, Zhao T, Xu B, Zhang F, Liu L, Tang J, Zhang G, Deng X, Chen F, *et al.* 2012. The histone methyltransferase SDG724 mediates H3K36me2/3 deposition at MADS50 and RFT1 and promotes flowering in rice. *Plant Cell* **24**: 3235–3247.
Tamaki S, Matsuo S, Wong HL, Yokoi S, Shimamoto K. **2007**. Hd3a Protein Is a Mobile. *Science* **316**: 1033–1036.
Tamaki S, Tsuji H, Matsumoto A, Fujita A, Shimatani Z, Terada R, Sakamoto T, Kurata T, Shimamoto K, Robert LF. **2015**. FT-like proteins induce transposon silencing in the shoot apex during floral induction in rice. *Proceedings of the National Academy of Sciences of the United States of America* **112**: E901–E910.
Taoka KI, Ohki I, Tsuji H, Furuita K, Hayashi K, Yanase T, Yamaguchi M, Nakashima C, Purwestri YA, Tamaki S, *et al.* 2011. 14-3-3 proteins act as intracellular receptors for rice Hd3a florigen. *Nature* **476**: 332–335.
Taoka K, Ohki I, Tsuji H, Furuita K, Hayashi K, Yanase T, Yamaguchi M, Nakashima C, Toriba T, Tokunaga H, Shiga T, Nie F, Naramoto S, Honda E, Tanaka K, Taji T, Itoh JI, Kyozuka J. **2019**. BLADE-ON-PETIOLE genes temporally and developmentally regulate the sheath to blade ratio of rice leaves. *Nature communications* **10**.
Tsuji H, Tachibana C, Tamaki S, Taoka K-I, Kyozuka J, Shimamoto K. **2015**. Hd3a promotes lateral branching in rice. *The Plant journal : for cell and molecular biology* **82**: 256–66.
Tsuji H, Taoka KI, Shimamoto K. **2013**. Florigen in rice: Complex gene network for florigen transcription, florigen activation complex, and multiple functions. *Current Opinion in Plant Biology* **16**: 228–235.
Ühlken C, Horvath B, Stadler R, Sauer N, Weingartner M. **2014**. MAIN-LIKE1 is a crucial factor for correct cell division and differentiation in Arabidopsis thaliana. *Plant Journal* **78**: 107–120.
Wang H, Tu R, Sun L, Wang D, Ruan Z, Zhang Y, Peng Z, Zhou X, Fu J, Liu Q, *et al.* 2022. Tiller Angle Control 1 Is Essential for the Dynamic Changes in Plant Architecture in Rice. *International Journal of Molecular Sciences 2022, Vol. 23, Page 4997* **23**: 4997.

Xu G, Ma H, Nei M, Kong H. **2009**. Evolution of F-box genes in plants: Different modes of sequence divergence and their relationships with functional diversification. *Proceedings of the National Academy of Sciences of the United States of America* **106**.
Yu B, Lin Z, Li H, Li X, Li J, Wang Y, Zhang X, Zhu Z, Zhai W, Wang X, *et al.* 2007. TAC1, a major quantitative trait locus controlling tiller angle in rice. *Plant Journal* **52**: 891–898.
Zhang L ZFZXPTXLSJYLSSYHCY. **2022**. The tetratricopeptide repeat protein OsTPR075 promotes heading by regulating florigen transport in rice. *Plant Cell* **Sep 27**: 3632-3646.
Zhao J, Chen H, Ren D, Tang H, Qiu R, Feng J, Long Y, Niu B, Chen D, Zhong T, *et al.* 2015. Genetic interactions between diverged alleles of Early heading date 1 (Ehd1) and Heading date 3a (Hd3a)/ RICE FLOWERING LOCUS T1 (RFT1) control differential heading and contribute to regional adaptation in rice (Oryza sativa). *New Phytologist* **208**: 936–948.
Zhu W, Yang L, Wu D, Meng Q, Deng X, Huang G, Zhang J, Chen X, Ferrándiz C, Liang W, *et al.* 2022. Rice SEPALLATA genes OsMADS5 and OsMADS34 cooperate to limit inflorescence branching by repressing the TERMINAL FLOWER1-like gene RCN4. *New Phytologist* **233**.

FIGURE 1

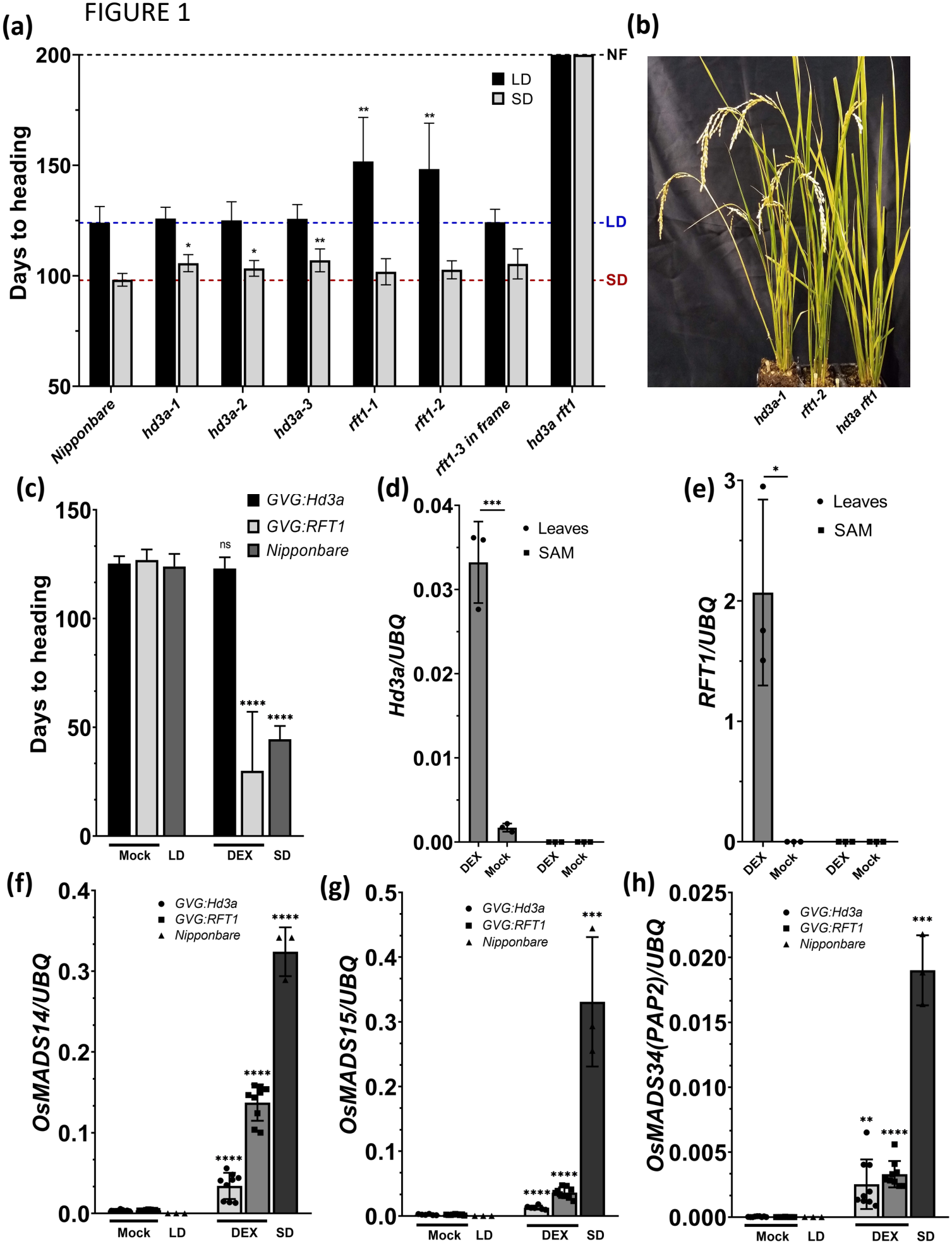

FIGURE 2

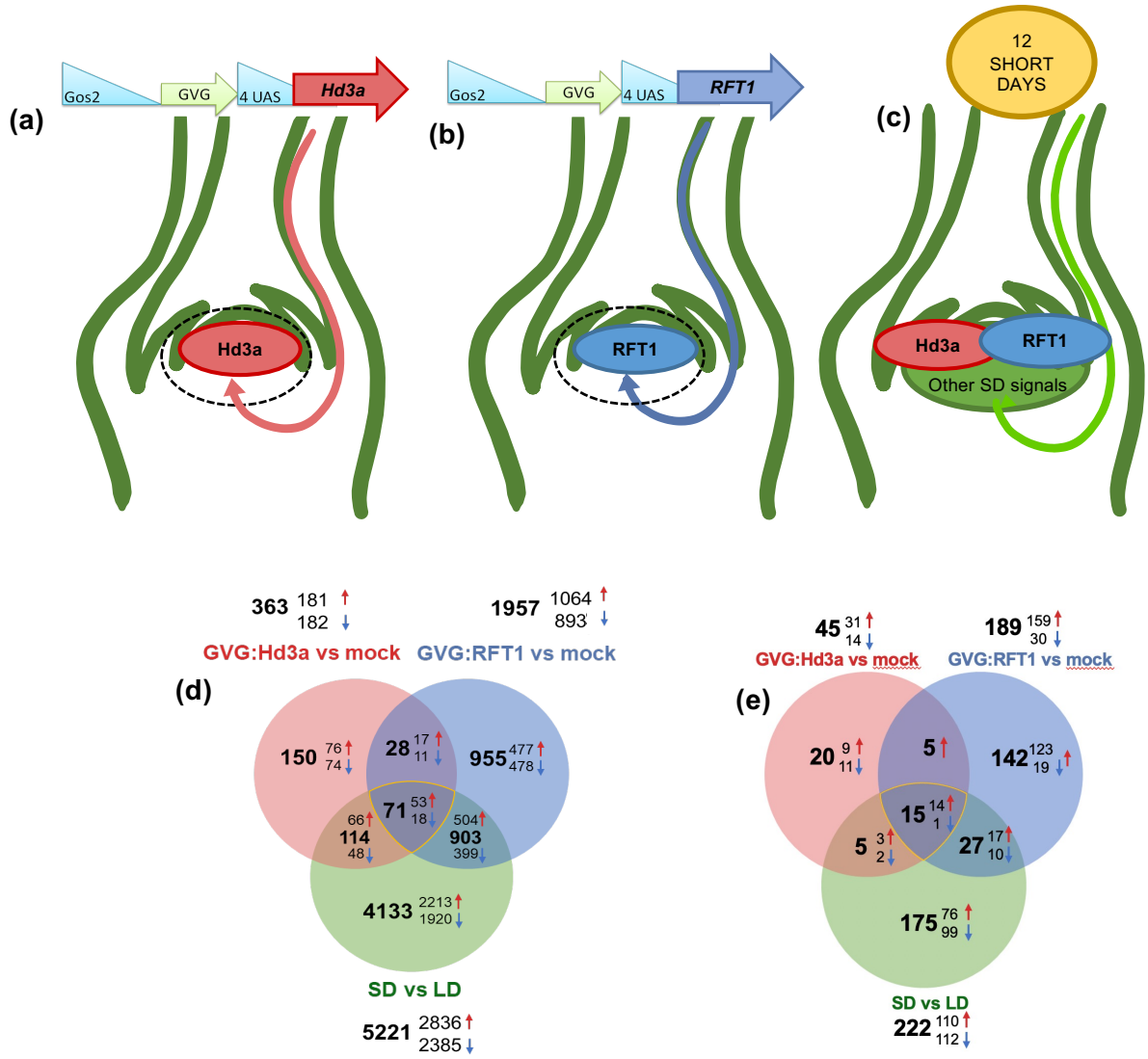

(f)

LOCUS ANNOTATION	GENE NAME	Log2FC Hd3a	Log2FC RFT1	Log2FC SD
LOC_Os07g01820	*OsMADS15*	6,79	8,29	8,87
LOC_Os04g29310	*retrotransposon HELICASE-RELATED/ nucleic acid binding/AT hook motif*	5,59	6,05	4,96
LOC_Os03g54160	*OsMADS14*	5,14	6,39	6,72
LOC_Os01g11940	*OsFT-Like1*	4,41	5,33	6,14
LOC_Os03g54170	*PANICLE PHYTOMERE 2 (PAP2)/OsMADS34*	4,27	5,53	6,49
LOC_Os08g13680	*retrotransposon HELICASE-RELATED*	3,48	4,58	3,52
LOC_Os04g48290	*MATE efflux membrane protein*	3,02	2,30	2,24
LOC_Os12g36680	*expressed protein*	2,46	5,25	3,15
LOC_Os08g37070	*expressed protein*	2,22	3,62	1,64
LOC_Os05g28210	*small hydrophilic plant seed protein/ Late Embryogenesis Abundant (LEA)*	2,21	4,87	3,94
LOC_Os01g09450	*Auxin-responsive Aux/IAA/ARF OsIAA2*	2,09	1,90	1,79
LOC_Os07g41370	*OsMADS18*	1,90	2,19	1,98
LOC_Os07g32406	*Similar to MAIN-LIKE1/plant mobile protein + serine/threonine phosphatase*	1,71	4,64	1,82
LOC_Os04g13150	*BROADER TILLER ANGLE 1 (BRT1) OsFBX125 - F-box domain*	1,51	2,35	3,48
LOC_Os12g42250	*PREMATURE INTERNODE ELONGATION 1 (PINE1)*	-1,36	-1,90	-2,45
LOC_Os01g04750	*AP2-B3 DNA binding domain*	-1,55	-1,62	-3,65

FIGURE 3

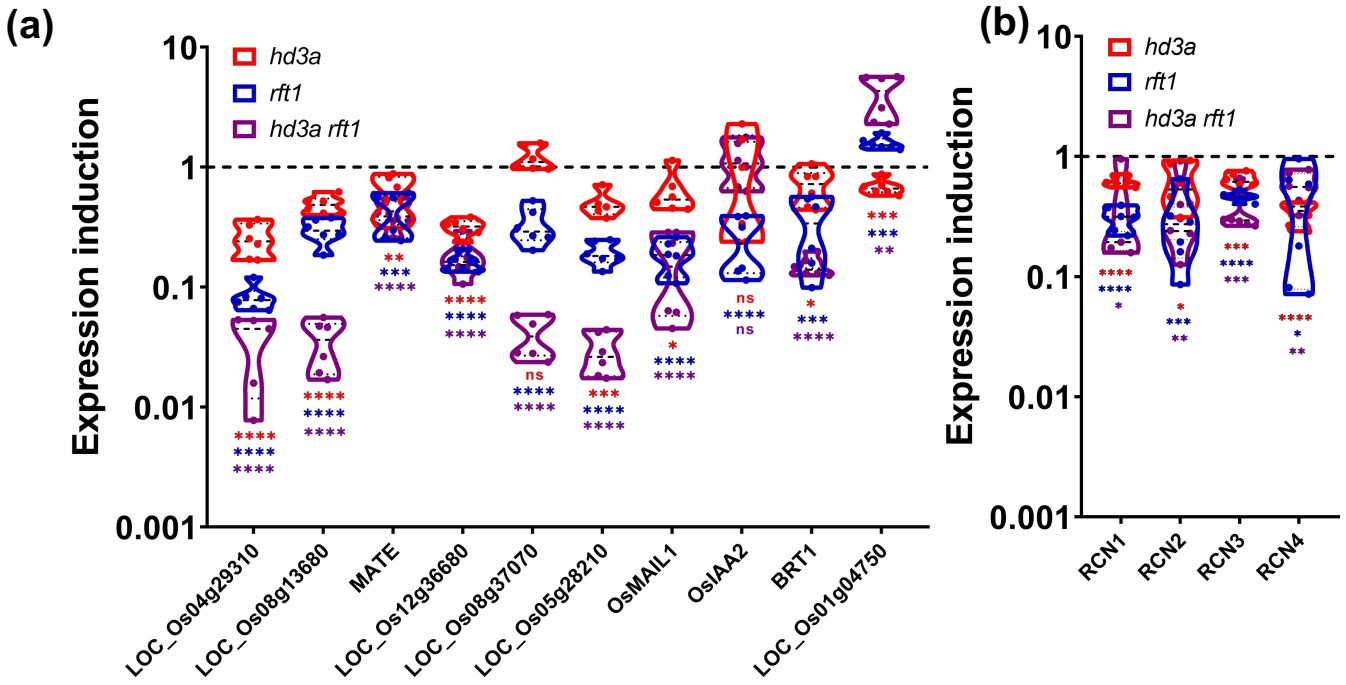

FIGURE 4